Hepatoprotective Effects of Indole, a Gut Microbial Metabolite, in Leptin-Deficient Obese Mice

Christelle Knudsen, Audrey Neyrinck, Quentin Leyrolle, Pamela Baldin, Sophie Leclercq, Julie Rodriguez, Martin Beaumont, Patrice Cani, Laure Bindels, Nicolas Lanthier, et al.

The Journal of Nutrition
Nutrition and Disease

Hepatoprotective Effects of Indole, a Gut Microbial Metabolite, in Leptin-Deficient Obese Mice

Christelle Knudsen,[1,2] Audrey M Neyrinck,[1] Quentin Leyrolle,[1] Pamela Baldin,[3] Sophie Leclercq,[1,4] Julie Rodriguez,[1] Martin Beaumont,[2] Patrice D Cani,[1,5] Laure B Bindels,[1] Nicolas Lanthier,[6,7] and Nathalie M Delzenne[1]

[1]Metabolism and Nutrition Research Group, Louvain Drug Research Institute, UCLouvain, Université catholique de Louvain, Brussels, Belgium; [2]GenPhySE, Université de Toulouse, INRAE, ENVT, 31320, Castanet Tolosan, France; [3]Service d'Anatomie Pathologique Cliniques Universitaires Saint-Luc, Brussels, Belgium; [4]Institute of Neuroscience, UCLouvain, Université catholique de Louvain, Brussels, Belgium; [5]WELBIO–Walloon Excellence in Life Sciences and BIOtechnology, UCLouvain, Université catholique de Louvain, Brussels, Belgium; [6]Service d'Hépato-gastroentérologie, Cliniques universitaires Saint-Luc, Brussels, Belgium; and [7]Laboratory of Gastroenterology and Hepatology, Institut de Recherche Expérimentale et Clinique, UCLouvain, Université catholique de Louvain, Brussels, Belgium

ABSTRACT

Background: The gut microbiota plays a role in the occurrence of nonalcoholic fatty liver disease (NAFLD), notably through the production of bioactive metabolites. Indole, a bacterial metabolite of tryptophan, has been proposed as a pivotal metabolite modulating inflammation, metabolism, and behavior.

Objectives: The aim of our study was to mimic an upregulation of intestinal bacterial indole production and to evaluate its potential effect in vivo in 2 models of NAFLD.

Methods: Eight-week-old leptin-deficient male *ob/ob* compared with control *ob/+* mice (experiment 1), and 4–5-wk-old C57BL/6JRj male mice fed a low-fat (LF, 10 kJ%) compared with a high-fat (HF, 60 kJ%) diet (experiment 2), were given plain water or water supplemented with a physiological dose of indole (0.5 mM, $n \geq 6$/group) for 3 wk and 3 d, respectively. The effect of the treatments on the liver, intestine, adipose tissue, brain, and behavior was assessed.

Results: Indole reduced hepatic expression of genes involved in inflammation [C-C motif chemokine ligand 2 (*Ccl2*), C-X-C motif chemokine ligand 2 (*Cxcl2*); 3.3- compared with 5.0-fold, and 2.4- compared with 3.3-fold of control *ob/+* mice, respectively, $P < 0.05$], and in macrophage activation [*Cd68*, integrin subunit α X (*Itgax*); 2.1- compared with 2.5-fold, and 5.0- compared with 6.4-fold of control *ob/+* mice, respectively, $P < 0.01$] as well as markers of hepatic damage (alaninine aminotransferase; −32%, $P < 0.001$) regardless of genotype in experiment 1. Indole had no effect on hepatic inflammation in mice fed the LF or HF diet in experiment 2. Indole did not change hepatic lipid content, anxiety-like behavior, or inflammation in the ileum, adipose tissue, and brain in experiment 1.

Conclusions: Our results support the efficacy of indole to reduce hepatic damage and associated inflammatory response and macrophage activation in *ob/ob* mice. These modifications appear to be attributable to direct effects of indole on the liver, rather than through effects on the adipose tissue or intestinal barrier. *J Nutr* 2021;151:1507–1516.

Keywords: gut-liver axis, microbiota, *ob/ob* mice, steatosis, tryptophan

Introduction

Concurrently with the increase in obesity and metabolic syndromes, nonalcoholic fatty liver disease (NAFLD) is becoming the most important cause of chronic liver disease, with a global prevalence of 24%. However, no pharmacological therapy is currently available (1). Diet plays an important role in the development of NAFLD, but growing evidence suggests that the gut microbiota also has its part to play in the occurrence and evolution of this disease, notably through the production of specific bioactive metabolites (2, 3). Most known bacterial metabolites are derived from dietary carbohydrates such as SCFAs, from dietary lipids such as PUFA-derived metabolites or bile acids, or from dietary proteins and amino acids such as indoles or phenols (3, 4). Due to its close anatomical proximity with the digestive tract, the liver can easily be reached by metabolites transiting from the gut lumen through the portal vein. Amino acid–derived metabolites such as phenylacetic acid (5), imidazole propionate (6), and 3-(4-hydroxyphenyl)lactate (7) are in the spotlight and have been identified as potential inducers of steatosis and hepatic inflammation whereas others,

Manuscript received August 28, 2020. Initial review completed October 30, 2020. Revision accepted January 28, 2021.
First published online March 10, 2021; doi: https://doi.org/10.1093/jn/nxab032.

such as indolic compounds, seem to preserve liver integrity (8–11).

Indole is a product of L-tryptophan deamination catalyzed by the bacterial enzyme tryptophanase. It is the main bacterial metabolite derived from tryptophan in the gut (12, 13), and it can be detected in healthy human and mouse feces at concentrations close to millimolar (12–15). In gnotobiotic rats, and at high doses [500 mg/kg body weight (BW)] in conventional rats, indole has been shown to modulate behavior, including anxiety-like and depression-like behaviors (16), and response to chronic mild stress (17). Conversely, at the intestinal level, indole decreases mucosal inflammation in vivo (at 20 mg/kg BW) and in vitro (at 1 mM) (18, 19) and enhances epithelial barrier function (at 20 mg/kg BW) (20). Indole (1 mM) can also modulate intestinal cell metabolism in vitro resulting in a change in glucagon-like peptide-1 secretion (21). Due to the close anatomical proximity between the intestine and the liver, the immunomodulatory effects of indole on gut barrier and intestinal immune response and inflammation (18, 20) could potentially impact the liver. Recent studies conducted by our laboratory have shown direct effects of indole on the liver with a reduction in inflammatory markers ex vivo and in vivo after an acute LPS challenge (8). This mechanistic study demonstrated that the anti-inflammatory effects of indole were partly dependent on Kupffer cells (KCs) and associated with a downregulation of key proteins of the NF-κB pathway. In this model, microarray analyses highlighted modulations of the expression of genes regulating specific metabolic pathways, including cholesterol metabolism. Thus, indole appears as a potential therapeutic tool for NAFLD treatment. In accordance with this hypothesis, a recent article reported that the concentration of circulating indole was inversely associated with the BMI and with the degree of liver lipid accumulation in humans, and that a high dose of indole (50 mg/kg) given over 3 wk decreased hepatic inflammation and steatosis in diet-induced obese mice (22). A large spectrum of Gram-negative and Gram-positive bacteria produce indole at variable levels (23). However, no data are currently available on the direct and indirect (mediated by the intestine and adipose tissue) impact of an upregulation of the bacterial indole production on hepatic health and metabolism. The aim of our study was thus to mimic an upregulation of intestinal bacterial indole production (chronic treatment with a low dose) and evaluate its impact on the liver, intestine, adipose tissue, and brain and on behavior. The model of genetic leptin deficiency was chosen because previous data support the decrease in proinflammatory cytokine expression in *ob/ob* liver slices upon incubation with indole (8). The impact of indole was also evaluated in a short-term dietary challenge model with a high-fat diet, that we previously established (24), to determine the potential preventive properties of an upregulation of bacterial indole production on the onset of hepatic disorders.

Methods

In vivo experiments

All mice were purchased from Janvier Labs and housed in a specific opportunistic pathogen–free environment. Housing conditions were as specified by the Belgian law of May 29, 2013 on the protection of laboratory animals (Agreement LA 1,230,314). Animals were placed in individually ventilated cages with bedding (Rehofix Corncob bedding MK1500; Technilab-BMI) in groups of 3. Hygrometry and temperature were monitored, and a 12- h daylight cycle was applied. Housing was enriched with a plastic tunnel for the mice to hide and a soft paper tissue. Bedding and tissues were changed weekly. Mice had free access to water and food [AIN-93M (25), D10012Mi; Research Diets] for 10–15 d before experiment. The experiments performed in this study were approved by the local Ethics Committee under the number 2017/UCL/MD/005.

Experiment 1.

Eighteen B6.V-Lep *ob*/+ JRj and 18 B6.V-Lep *ob/ob* JRj 8-wk-old male mice were randomly allocated (9 mice/group; **Figure 1**A) to either receive water with no supplementation (*ob*/+ C and *ob/ob* C mice) or water supplemented with indole (*ob*/+ I and *ob/ob* I mice) (Sigma; dosage as specified below). Standard diet [AIN93M, 9%kJ fat (25), D10012Mi; Research Diets] and water was provided *ad libitum*. Behavioral tests were performed after 2 wk of experiment using the light-dark box test (see **Supplemental Methods**). Diet and mice were weighed twice a week, whereas water was weighed daily.

After 3 wk of experiment and 4 h of fasting, 20 μL of blood were sampled at the tail vein for further insulin measurements, and glycemia was measured using a glucometer (Roche Diagnostics). After 6h of fasting the mice were anesthetized with isofluorane gas (Forene; Abbott) for blood samplings. Mice were then killed by cervical dislocation, and liver, ileum, brain, kidneys, cecal tissue and content, and subcutaneous, visceral, and epididymal adipose tissues were collected. All organs, with the exception of blood, brain, and ileum, were weighed. For the detection of neutral lipids, 2 sections of the left lateral and right medial lobes of the liver were stained using Oil Red O. NAFLD severity was evaluated on hematoxylin and eosin (H&E) stains of similar liver sections (see Supplemental Methods for details of histological measurements).

The rest of the liver was snap frozen in liquid nitrogen and stored at −80°C until analysis. The subcutaneous adipose tissue and a 1-cm section of the ileum were sampled, frozen in liquid nitrogen, and stored at −80°C until analysis. Peripheral blood was collected in an EDTA-coated tube and centrifuged at 13,000 × *g* for 3 min at 4°C, then plasma was collected and stored at −80°C until analysis. Frontal cortex and striatum were quickly dissected and incubated in RNAlater (Life

CK is a beneficiary of the AgreenSkills+ fellowship program, which has received funding from the EU's Seventh Framework Programme under grant agreement N°FP7-609398 (AgreenSkills+ contract). PDC is a senior research associate at FRS-FNRS (Fonds de la Recherche Scientifique) and recipient of grants from FNRS (WELBIO-CR-2019C-02R, "The Excellence of Science: EOS 30770923") and the Funds Baillet Latour (Grant for Medical Research 2015). NMD is a recipient of grants from SPW-EER (convention 1610365, ERA-HDHL cofunded call BioNH 2016), from the Fonds de la Recherche Scientifique (FRS-FNRS) [PINT-MULTI R.8013.19 (NEURON-ERANET, call 2019) and PDR T.0068.19], and from the Fédération Wallonie-Bruxelles (Action de Recherche Concertée ARC18-23/092).

Author disclosures: The authors report no conflicts of interest.

Supplemental Figures 1–4, Supplemental Tables 1–5, and Supplemental Methods are available from the "Supplementary data" link in the online posting of the article and from the same link in the online table of contents at https://academic.oup.com/jn/.

Address correspondence to NMD (e-mail: nathalie.delzenne@uclouvain.be).

Abbreviations used: *Adgre1*, adhesion G protein-coupled receptor E1; AhR, aryl hydrocarbon receptor; Akt, protein kinase B; ALAT, alanine aminotransferase; ASAT, aspartate aminotransferase; BW, body weight; *Ccl*, C-C motif chemokine ligand; *Col1a1*, collagen type I α 1 chain; *Cxcl*, C-X-C motif chemokine ligand; *Cyp1a1*, cytochrome P450 family 1 subfamily A polypeptide 1; *Cyp1b1*, cytochrome P450 family 1 subfamily B polypeptide 1; FA, fatty acid; FFA, free fatty acid; H&E, hematoxylin and eosin; HF, high-fat diet; HF C, control high-fat-diet–fed mice in experiment 2; HF I, indole-treated high-fat-diet–fed mice in experiment 2; IKBA, NF-κB inhibitor α; *Itgax*, integrin subunit α X (*Cd11c*); KC, Kupffer cell; LF, low-fat diet; LF C, control low-fat-diet–fed mice in experiment 2; LF I, indole-treated low-fat-diet–fed mice in experiment 2; MTOR, mechanistic target of rapamycin; MTORC, mechanistic target of rapamycin complex; NAFLD, nonalcoholic fatty liver disease; NEFA, non-esterified fatty acid; *ob*/+ C, control *ob*/+ mice in experiment 1; *ob*/+ I, indole-treated *ob*/+ mice in experiment 1; *ob/ob* C, control *ob/ob* mice in experiment 1; *ob/ob* I, indole-treated *ob/ob* mice in experiment 1; PLS-DA, partial least squares discriminant analysis.

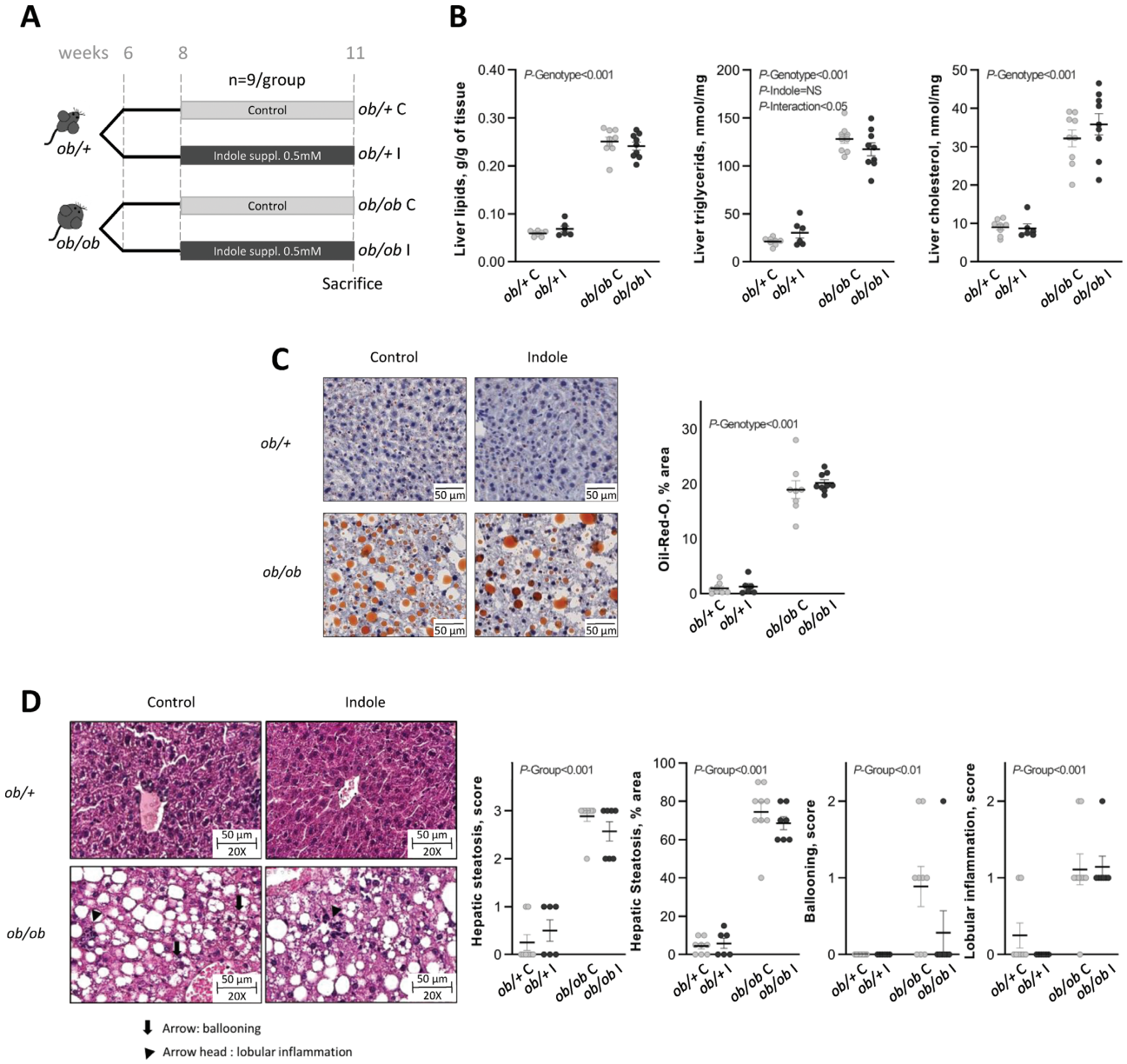

FIGURE 1 Effect of indole supplementation (0.5 mM) in *ob/+* and *ob/ob* mice for 3 wk (A: experiment 1) on (B) hepatic lipids and (C, D) hepatic histology. (C) Representative Oil Red O (ORO)-stained liver sections for each experimental group (bar = 50 μm) and mean ORO relative area per group. Two-factor ANOVA was used with genotype and indole treatment as fixed effects and the cage as random effect. (D) Representative H&E-stained liver sections for each experimental group, ballooning being signaled by an arrow and lobular inflammation by an arrow head. Scoring was performed on 3 criteria: steatosis (0–3 and % area), ballooning (0–2), and lobular inflammation (0–2). Scoring was analyzed using a nonparametric Kruskal–Wallis test with the experimental group as factor. Data are presented as means ± SEM, $n \geq 6$/group. H&E, hematoxylin and eosin; NS, not significant ($P \geq 0.05$); *ob/+* C, control *ob/+* mice; *ob/+* I, indole-treated *ob/+* mice; *ob/ob* C, control *ob/ob* mice; *ob/ob* I, indole-treated *ob/ob* mice; suppl., supplemented.

Technologies, Invitrogen) overnight at 4°C, then transferred at −20°C until analysis.

Experiment 2.

Twenty-four C57BL/6JRj male mice (4–5 wk old) were either fed a low-fat (10%kJ fat, labeled LF) or high-fat diet (60%kJ fat, labeled HF; Ssniff, Soest; see **Supplemental Table 1** for chemical composition) and randomly allocated (6 mice/group; **Supplemental Figure 1**A) to receive either plain water (LF C and HF C mice) or water supplemented with indole (0.5 mM; LF I and HF I mice). Food and water was provided *ad libitum*. Diet and water intake as well as BW were recorded daily. After 3 d of experiment, the mice were anesthetized with isoflurane gas (Forene; Abbott) in the morning for blood samplings. Mice were then killed by cervical dislocation and liver, subcutaneous, visceral, and epididymal adipose tissues were collected. All organs were weighed. Samples were taken and stored as specified for experiment 1.

Dosage information

Indole was provided in the drinking water at a dose of 0.5 mM [solubility of 30 mM at 25°C (26)]. We took into account the daily water intake to calculate the estimated indole intakes of *ob/ob* I and *ob/+* I mice (mean values of 8 to 10 mg/kg, Table 1) as well as LF I and HF I mice (mean values of 13 to 16 mg/kg). Indole being a photosensitive molecule, fresh indole solutions were prepared daily.

TABLE 1 Effect of indole on feeding behavior and morphological parameters in *ob/+* and *ob/ob* mice in experiment 1[1]

	ob/+		*ob/ob*		*P* value[2]		
	ob/+ C ($n = 8$)	*ob/+* I ($n = 6$)	*ob/ob* C ($n = 9$)	*ob/ob* I ($n = 9$)	Genotype	Indole	G × I
Initial BW (8 wk), g	25.4 ± 2.2	25.9 ± 2.8	39.9 ± 4.0	40.5 ± 5.0	***	NS	NS
Final BW (11 wk), g	28.1 ± 2.4	28.4 ± 2.2	43.0 ± 3.6	43.8 ± 4.4	***	NS	NS
BW gain, g	2.67 ± 0.84	2.56 ± 1.27	3.10 ± 1.20	3.29 ± 1.49	NS	NS	NS
Liver weight/BW, %	3.57 ± 0.21	3.64 ± 0.21	6.46 ± 0.71	5.86 ± 1.12	***	NS	NS
White adipose tissue							
Subcutaneous adipose tissue/BW, %	2.32 ± 0.49	2.50 ± 0.51	7.64 ± 0.60	7.71 ± 0.43	***	NS	NS
Visceral adipose tissue/BW, %	1.18 ± 0.24	1.19 ± 0.17	2.48 ± 0.30	2.36 ± 0.48	***	NS	NS
Epididymal adipose tissue/BW, %	2.63 ± 0.37	2.85 ± 0.44	6.64 ± 0.68	6.08 ± 0.57	***	NS	NS
Cecal tissue/BW, %	0.25 ± 0.02	0.25 ± 0.01	0.15 ± 0.02	0.16 ± 0.04	***	NS	NS
Cecal content/BW, %	0.61 ± 0.15	0.71 ± 0.06	0.27 ± 0.08	0.27 ± 0.07	***	NS	NS
Kidney weight/BW, %	1.02 ± 0.05	0.98 ± 0.07	0.75 ± 0.13	0.71 ± 0.15	***	NS	NS
Diet intake, g/day	2.88 ± 0.34	3.02 ± 0.29	3.68 ± 0.21	3.21 ± 0.17	*	NS	NS
Total estimated indole intake, mg/kg BW	—	10.5 ± 2.0	—	8.1 ± 3.1	NS		

[1]Two-way ANOVA was used with genotype and indole treatment as fixed effects and the cage as random effect. Data are presented as means ± SD, $n \geq 6$/group. BW, body weight; G × I, interaction between genotype and indole treatment; NS, not significant; *ob/+* C, control *ob/+* mice; *ob/+* I, indole-treated *ob/+* mice; *ob/ob* C, control *ob/ob* mice; *ob/ob* I, indole-treated *ob/ob* mice.
[2]NS, $P \geq 0.05$; $^{*}P < 0.05$; $^{***}P < 0.001$.

Biochemical analyses

Plasma triglycerides, cholesterol, and nonesterified fatty acid (NEFA) concentrations were measured using kits coupling enzymatic reactions and spectrophotometric detections (SpectraMax i3x; Molecular Devices) of end products (Diasys Diagnostic and Systems). Total lipid content was measured in the liver after extraction with chloroform-methanol according to the Folch method as previously described (27). Triglycerides and cholesterol were measured in the liver (Diasys Diagnostic and Systems). Alanine aminotransferase (ALAT) and aspartate aminotransferase (ASAT) concentrations were measured (SpectraMax i3x; Molecular Devices) in the plasma as markers of liver damage using commercial kits according to the manufacturer's instructions (Diasys Diagnostic and Systems). Plasma insulin concentrations were determined (SpectraMax i3x; Molecular Devices) using an ELISA kit (Mercodia) on the blood collected at the tail vein.

Tissue mRNA analyses

Total RNA was isolated from tissues using TriPure Isolation Reagent (Roche Diagnostics). cDNA was prepared by reverse transcription of 1 μg total RNA using the Reverse Transcription System (Promega). Real-time PCR was performed with a QuantStudio 3 Real-Time PCR System (Applied Biosystems) using MasterMix GoTaq (Promega). Data were analyzed according to the 2-ΔΔCT method. The purity of the amplified products was verified by analyzing the melting curve obtained at the end of the amplification step. The ribosomal protein L19 (*Rpl19*) gene was used as reference gene. Sequences of primers used are listed in **Supplemental Table 2**.

Western blots (experiment 1)

Western blot analyses on liver samples were performed as previously described (8) for the NF-κB and protein kinase B/mechanistic target of rapamycin (AKT/MTOR) signaling pathways [primary antibodies detecting respectively NF-κB p65, phospho-NF-κB p65 (Ser536), NF-κB inhibitor α (IKBA) and phospho-IKBA (Ser32), AKT, phospho-AKT (Ser473), MTOR and phospho-MTOR (Ser2448); Cell Signaling Technology). beta-actin was used as control protein (Abcam). Signals were revealed using the SuperSignal West Pico substrate with Femto Chemiluminescent substrate addition for the NF-κB pathway (Thermo Fisher Scientific), and analyzed with the ImageQuant TL instrument and software v.8.1 (GE Healthcare).

Statistical analyses and graphical output

In experiment 1, four B6.V-Lep *ob/+* JRj mice (1 *ob/+* C and 3 *ob/+* I mice) presented abnormal hepatic and metabolic profiles with high cellular and hepatic damage at the end of the experiment associated with high urinary bilirubin concentrations before the onset of experimental procedures and were thus excluded from all analyses.

All data were analyzed using R 3.4.3 software (R Foundation). H&E histology scoring was analyzed using a nonparametric Kruskal–Wallis test with the experimental group as factor. When significant ($P < 0.05$), groups were compared pairwise with a Wilcoxon test. For all other variables, to verify homoscedasticity of the data, a Levene test was performed, and data were log transformed when needed. qPCR data being log normally distributed (asymmetrical distribution), the log transformation was applied systematically for these kind of data. A linear mixed model followed by a 2-way ANOVA was used with indole treatment and genotype (experiment 1) or diet (experiment 2) as fixed effects and the cage as random effect. Pairwise comparisons within each genotype (*ob/+* C compared with *ob/+* I, and *ob/ob* C compared with *ob/+* I) or diet (LF C compared with LF I, and HF C compared with HF I) were performed using a Tukey post hoc test. In experiment 1, to have an overview of the general trends in the data sets, multivariate partial least squares discriminant analyses (PLS-DAs) were also performed using the mixOmics package (28, 29) on parameters related to hepatic damage, inflammation, macrophage activity, and fibrosis. The error rate (max. distance) was used to assess the performances of the analyses using the leave one out method according to the guidelines of the R mixOmics package (28). Using both genotypes the error rate was high (59.7%), and genotype was the main factor separating the individuals hiding treatment effect (**Supplemental Figure 2**), thus analyses were performed and presented separately for each genotype. For all statistical tests $P < 0.05$ was considered significant. Graphical outputs were obtained using GraphPad Prism 5 (GraphPad Software; univariate analyses) and R mixOmics package (multivariate analyses).

Results

Hepatoprotective effects of indole in *ob/ob* mice but not in a short-term model of HF diet–fed mice

As expected, *ob/ob* mice were >50% heavier than *ob/+* mice at the end of experiment 1 largely due to excessive adiposity (Table 1). Liver weight was also increased (Table 1). Higher plasma cholesterol and NEFAs and increased hepatic lipid, triglyceride, and cholesterol contents characterized *ob/ob* mice compared with *ob/+* mice (Figure 1B,C; **Supplemental Table 3**). *ob/+* mice had normal liver histology (Figure 1D), and indole did not alter liver morphology or lipid content, confirming the absence of deleterious effects of this molecule in the

absence of steatosis. In contrast, *ob/ob* mice were characterized by steatosis (predominantly macrovacuolar steatosis, but also microvesicular steatosis) with minimal ballooning and inflammation (Figure 1D). None of these traits were alleviated by a 3-wk indole treatment. Concurrently, indole did not change mRNA levels of hepatic genes involved in lipid metabolism in *ob/ob* mice, including those regulating *de novo* lipogenesis [acetyl-CoA carboxylase α (*Acaca*), fatty acid synthase (*Fasn*), MLX interacting protein like (*Mlxipl*, also known as *Chrebp*), and sterol regulatory element binding transcription factor 1 (*Srebf1*)], those involved in fatty acid (FA) oxidation [carnitine palmitoyltransferase 1A (*Cpt1a*)], FA transport (*Cd36* and microsomal triglyceride transfer protein (*Mttp*)], and bile acid metabolism [cytochrome P450 family 7 subfamily A and B members 1 (*Cyp7a1* and *Cyp7b1*), fibroblast growth factor 21 (*Fgf21*)] (Supplemental Table 3).

Interestingly, in experiment 1, indole reduced the concentration of serum ALAT regardless of genotype, whereas ASAT concentrations were not statistically significantly different despite a 50% numeric decrease in concentration as well (**Figure 2**A). PLS-DA analyses were performed separately in both genotypes on inflammatory, macrophage, and fibrotic markers to determine the most contributing markers to the discrimination between indole-treated and control mice. In *ob/+* mice the markers used had a good predictive ability (error rate = 8.3%). The discrimination was mainly driven by fibrosis marker collagen type I α 1 chain (*Col1a1*) and cell marker integrin subunit α X (*Itgax*, also known as *Cd11c*) (Figure 2B–D). In *ob/ob* mice the markers used had a poor predictive ability (error rate = 38.8%), and discrimination was mainly driven by monocyte chemoattractant protein 1 (*Mcp1*), also known as C-C motif chemokine ligand 2 (*Ccl2*), and C-X-C motif chemokine ligand 2 (*Cxcl2*) (Figure 2C–E). Univariate analyses demonstrated a significant modulation of these markers with a reduction in the expression of inflammatory markers *Ccl2* and *Cxcl2*, macrophage marker *Cd68*, cell marker *Itgax*, and fibrosis marker *Col1a1* with indole regardless of genotype (Figure 2F, **Supplemental Table 4**). The NF-κB pathway modulates the expression of several proinflammatory cytokines, including *Ccl2* (30). Western blot analyses showed that the phosphorylated/total IKBA ratio was increased in *ob/ob* mice, whereas phosphorylated/total NF-κB-p65 remained stable despite strong modulations of the inflammatory gene expression levels. No significant difference in the phosphorylated/total NF-κB-p65 ratio or the phosphorylated/total IKBA ratio occurred upon indole treatment (**Supplemental Figure 3**, Supplemental Table 4). The mechanistic target of rapamycin complex 1 (MTORC1) is also known to induce *Ccl2* expression through the forkhead box K1 (FOXK1) pathway (31). This pathway is also induced by insulin (31), but indole neither modulated the phosphorylated/total MTOR and protein kinase B (AKT) ratios nor plasma insulin concentrations (Supplemental Tables 3 and 4; Supplemental Figure 3). Aryl hydrocarbon receptor (AhR) ligands have been shown to have a protective role against genetic and high-fat diet–induced steatosis, hepatic damage, and inflammation (32, 33). Here we studied 2 key AhR target genes involved in the metabolism of xenobiotics, *Cyp1b1* and *Cyp1a1*. Indole downregulated the expression of *Cyp1b1* without impacting on *Cyp1a1* gene expression regardless of genotype (Figure 2G).

In experiment 2 we evaluated if indole could have a preventive effect on the establishment of a short-term diet-induced steatosis consisting of a 3-d administration of a high-fat diet (HF, 60% lard) (Supplemental Figure 1A). As expected, and as previously observed (24), obesogenic traits were observed, such as an increase in BW, visceral adipose tissue, liver lipids, and cholesterol and triglyceride concentrations after 3 d of HF diet feeding (Supplemental Figure 1B,C; **Supplemental Table 5**). This was also associated with hepatic inflammation (*Ccl2* and *Cxcl2* expression) and macrophage activation [*Cd68* and adhesion G protein-coupled receptor E1 (*Adgre1*) mainly] (Supplemental Figure 1E). Indole treatment neither prevented obesogenic traits nor modified transaminase concentrations, inflammation, and macrophage activation in the liver (Supplemental Figure 1D,E).

Effect of indole on extrahepatic tissues (gut, adipose tissue, and brain) and behavior in *ob/ob* mice

We evaluated whether the beneficial impact of indole on liver injury and inflammation in *ob/ob* I mice was mediated by a decreased permeability and inflammation in the ileum. Gene expression of tight junction protein 1 (*Tjp1*), occludin (*Ocln*), and mucin 2 (*Muc2*), contributing to epithelial protection, was not affected by indole treatment or genotype (**Figure 3**A). Only the expression level of tight junction gene claudin 2 (*Cldn2*), forming paracellular channels in the epithelia, was reduced in *ob/ob* mice, but indole did not alleviate this decrease. When looking at genes involved in the inflammatory response, such as interleukin 1 β (*Il1b*), tumor necrosis factor (*Tnf*), *Ccl2*, interferon gamma (*Ifng*), and interleukin 10 (*Il10*), no differences were observed between genotypes and treatments (Figure 3B,C). When analyzing lymphocyte markers in the gut, expression of the regulatory T cell marker forkhead box P3 (*Foxp3*) was differentially modulated by indole treatment in *ob/+* and *ob/ob* mice (*P*-interaction <0.05), whereas the T-lymphocyte marker CD3 antigen, gamma polypeptide (*Cd3g*) was unaffected by indole treatment. Concentrations of indoleamine 2,3-dioxygenase 1 (*Ido1*), involved in the immune response but also in the kynurenine pathway of tryptophan metabolism, were unaffected by both genotype and indole treatment (Figure 3C).

Adipose tissue cytokines and adipokines can also contribute to NAFLD development. Gene expression of proinflammatory chemokines *Ccl2* and *Cxcl2* and macrophage markers *Cd68* and *Adgre1* (*F4/80*) was increased in *ob/ob* mice, but indole did not alleviate this increase (Supplemental Table 4).

Because indole can have an impact on the brain, we wanted to evaluate whether a low dose of indole affected behavior and cerebral inflammatory processes. *ob/ob* mice are prone to anxiety-like-behavior (34), as confirmed in our light-dark box observations with a reduction of the time spent in the light, a shorter total distance moved, a reduced velocity, and a lower number of zone transitions (**Supplemental Figure 4**). None of these alterations were prevented, or worsened, with indole treatment. At the cerebral level, no drastic modulations of inflammatory genes were observed in *ob/ob* mice in the frontal cortex and the striatum, and indole did not affect their expression level regardless of genotype (Supplemental Table 4).

Discussion

Previous work from our laboratory demonstrated that indole reduces the hepatic inflammatory response to LPS in vitro and in an acute inflammatory LPS challenge in vivo (8). The present work adds to these prior results by evidencing the hepatoprotective properties of a low physiological dose of indole in a genetic

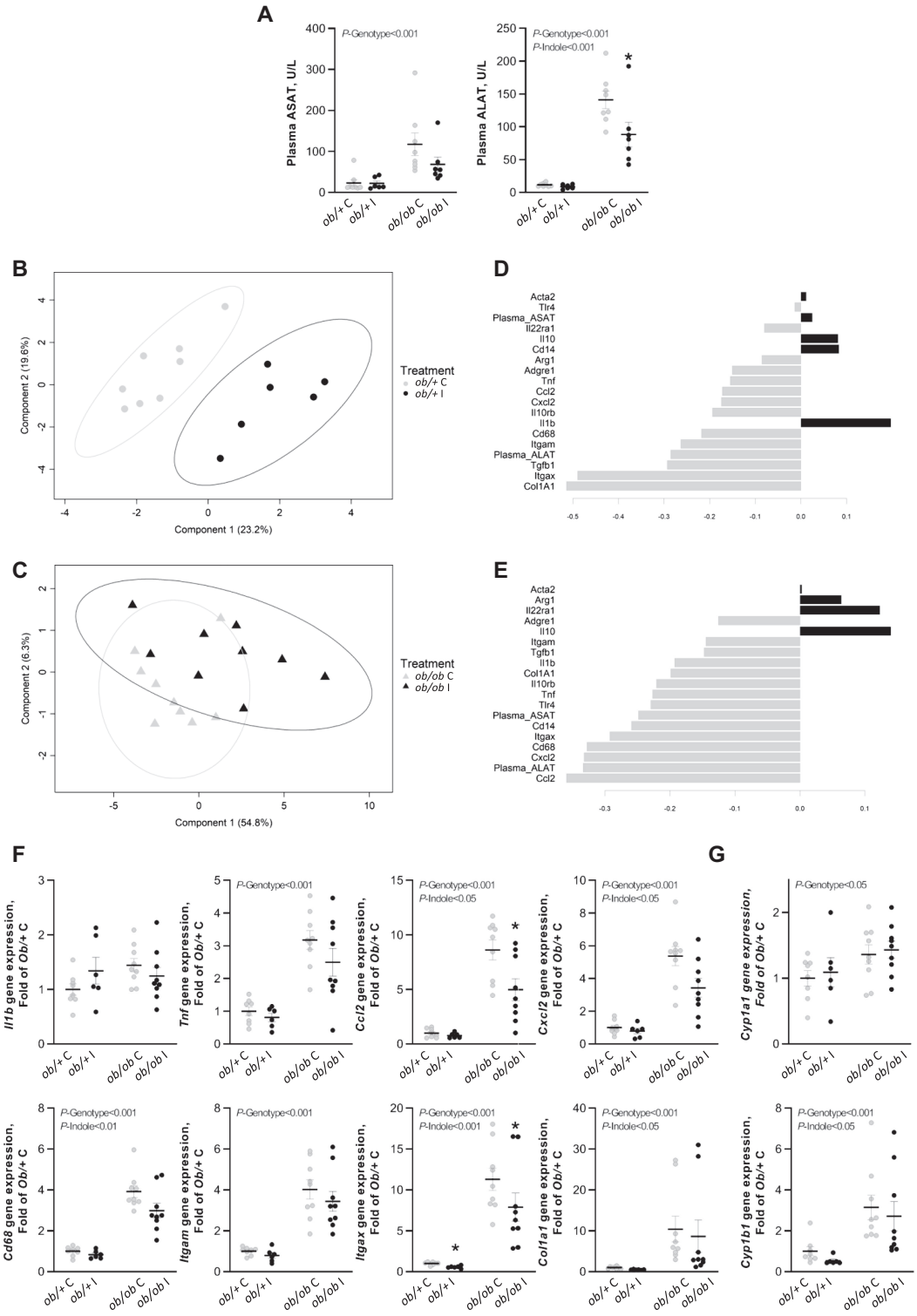

FIGURE 2 Effect of indole on (A) serum amino transferases and (B–G) hepatic gene expression in *ob/+* and *ob/ob* mice in experiment 1. PLS-DA analysis was performed on hepatic inflammatory and immune parameters in (B) *ob/+* [error rate (max. distance) = 8.3%] and (C) *ob/ob* mice [error rate (max. distance) = 38.8%]. In the sample scatter plots each dot/triangle represents a mouse. Mice can be discriminated according to treatment on component 1. Contribution level of the inflammatory and immune variables on component 1 for the (D) *ob/+* and (E) *ob/ob* mice. The bar length represents the importance of the variable in the multivariate model. Bars are colored according to the experimental group with the maximal mean expression level. (F, G) Two-way ANOVA was used with genotype and indole treatment as fixed effects and the cage as random effect. Mean values were compared pairwise using the Tukey post-hoc test. Data are presented as means ± SEM, $n \geq 6$/group. NS, not significant ($P \geq 0.05$); ∗significantly different from control within a genotype ($P < 0.05$). ALAT, alanine aminotransferase; ASAT, aspartate aminotransferase; *Ccl2*, C-C motif chemokine ligand 2; *Col1a1*, collagen type I α 1 chain; *Cxcl2*, C-X-C motif chemokine ligand 2; *Cyp1a1*, cytochrome P450 family 1 subfamily A polypeptide 1 ; *Cyp1b1*, cytochrome P450 family 1 subfamily B polypeptide 1; *Itgam*, integrin subunit α M (*Cd11b*); *Itgax*, integrin subunit α X (*Cd11c*); *ob/+* C, control *ob/+* mice; *ob/+* I, indole-treated *ob/+* mice; *ob/ob* C, control *ob/ob* mice; *ob/ob* I, indole-treated *ob/ob* mice; PLS-DA, partial least squares discriminant analysis.

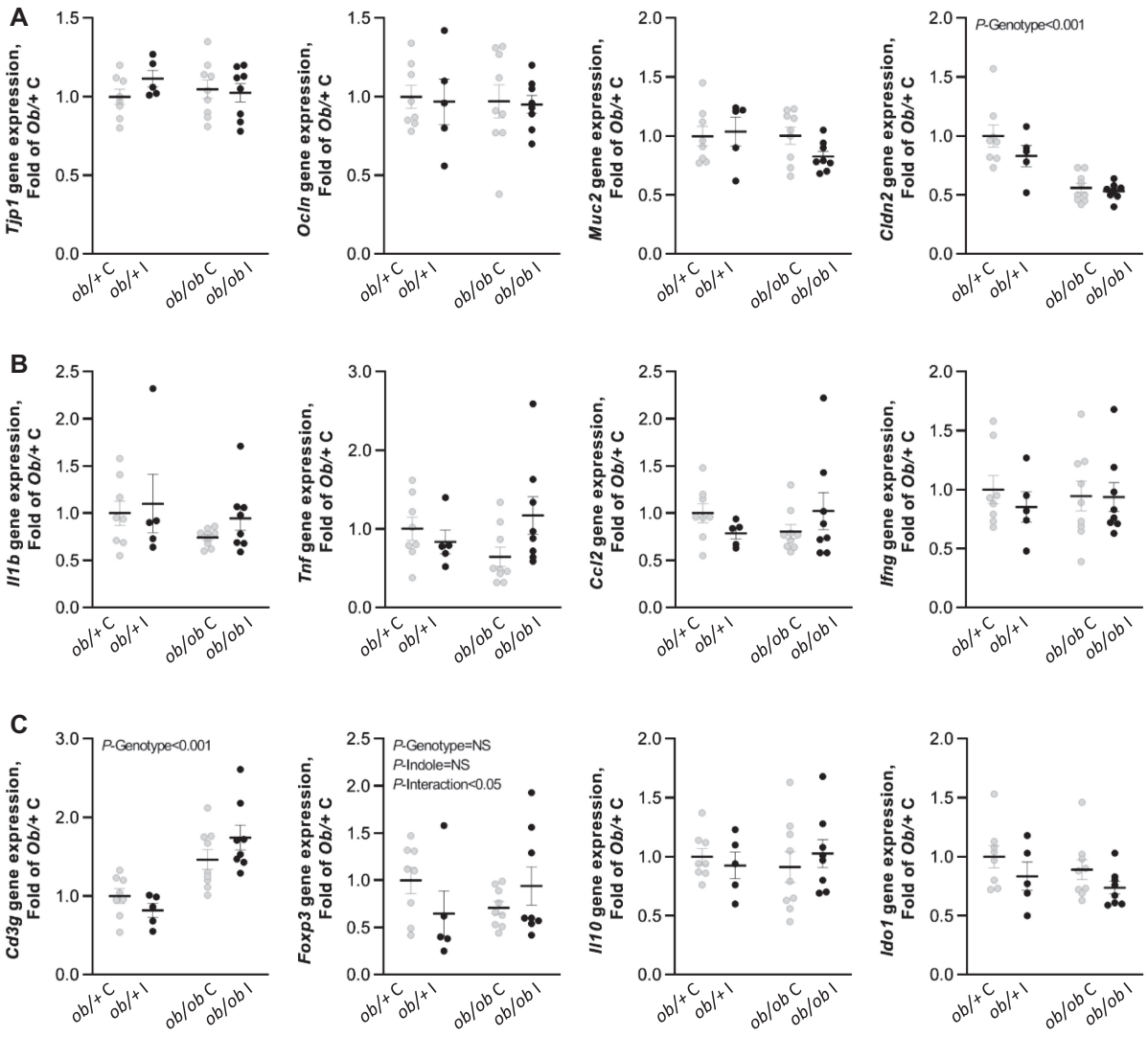

FIGURE 3 Effect of indole on gene expression levels implicated in (A) intestinal barrier function, (B) inflammation, and (C) immune response in the ileum in *ob/+* and *ob/ob* mice in experiment 1. Two-way ANOVA was used with genotype and indole treatment as fixed effects and the cage as random effect. Data are presented as means ± SEM, $n \geq 6$/group. *Ccl2*, C-C motif chemokine ligand 2; *Cldn2*, Claudin 2; *Foxp3*, Forkhead box P3; *Ido1*, Indoleamine 2,3-dioxygenase 1; *Ifng*, Interferon γ; *Muc2*, Mucin 2; NS, not significant ($P \geq 0.05$); *ob/+* C, control *ob/+* mice; *ob/+* I, indole-treated *ob/+* mice; *ob/ob* C, control *ob/ob* mice; *ob/ob* I, indole-treated *ob/ob* mice; *Ocln*, Occludin; *Tjp1*, Tight junction protein 1.

model of obesity and associated NAFLD, without improving steatosis and lipid homeostasis. It also suggests that indole acts directly on liver inflammation, without any intermediate regulation through the intestinal immune response and barrier function. Compared with previous studies (8, 18, 20, 35), our protocol presents the advantage of administering indole at lower and more physiologically relevant doses through the drinking water, representing a more physiological delivery mode over the course of the day, mainly centered around feed intake periods.

Macrophages play an important role in the regulation of inflammation and fibrogenesis in the liver. A 3-wk indole supplementation reduced the expression of *Cd68* and *Itgax* (also known as *Cd11c*) in lean and obese mice alike. *Itgax* is a marker of multiple immune cells, mainly dendritic and monocyte-derived cells and macrophages (36). It has been evidenced that CD11c+ hepatic macrophages could be prominent drivers of hepatocyte death–triggered liver fibrosis in nonalcoholic steatohepatitis (37). Thus, the reduction in *Itgax* with indole could indicate a decrease in CD11C+ activated macrophages consistent with the decrease in expression of fibrosis marker *Col1a1*. The reduced *Cd68* expression specifically suggests a reduced macrophage activity. These results accord with those of Ma et al. (22), who evidenced a reduced macrophage proinflammatory activation in the liver with indole (50 mg/kg) in diet-induced steatosis. However, it is important to note that indole was not effective in modulating inflammation in mice fed a high-fat diet for a few days, despite the fact that certain proinflammatory cytokines could be induced in this model.

The reduced *Ccl2* and *Cxcl2* expression levels observed with indole could indicate a reduced monocyte and neutrophil recruitment by KCs, the main resident macrophages in the liver. Upon liver injury these cells recruit circulating monocytes and neutrophils (38). Monocyte recruitment is mainly mediated by CCL2 secretions, whereas neutrophil recruitment is mediated

by CXCL1, CXCL2, and IL8 (CXCL8 in humans and CXCL15 in mice) (39). Upon liver injury, hepatocytes also secrete CCL2 (39). Its decreased expression could thus be in line with the lower hepatic damage with indole. Activated KCs, macrophage-derived monocytes, and neutrophils all induce increases in NF-κB and subsequent secretion of proinflammatory cytokines. Surprisingly, no significant reduction in the expression of proinflammatory cytokines was observed with indole in accordance with the absence of effect on NF-κB-p65 activation. The reduced macrophage and neutrophil activation could also explain the reduction in the expression of fibrosis marker *Col1a1* with indole (40, 41).

Indole and other indolic compounds have been shown to be AhR activators in vitro on human cell lines (42–44), potentially explaining the protective role against hepatic damage and inflammation. We have previously shown that precision-cut liver slices of *ob/ob* mice incubated with indole exhibited a higher expression of *Cyp1b1* and *Cyp1a1*, reflecting the activation of AhR (8). Here, in vivo in *ob/ob* mice, we show that indole treatment decreased *Cyp1b1* expression but did not affect *Cyp1a1*. However, the role of indole as an AhR activator is controversial (44). Thus, the anti-inflammatory effect of indole could be AhR-independent.

Inflammatory cytokines, notably *Ccl2*, can directly regulate hepatic lipid metabolism and induce triglyceride accumulation (45). No change in hepatic lipid metabolism was observed in our study with indole, unlike observations in diet-induced obese rodents with indole (22) and other indolic compounds, such as indole-3-propionic acid (10) and indole-3-acetic acid (11). This discrepancy could be linked to the low dose used in our study compared with the aforementioned ones (20–50 mg/kg compared with 8–10 mg/kg). Despite being a more physiological administration, supplying indole in the drinking water also induces variability in indole intake between animals, possibly explaining the variability in response obtained.

Hepatic macrophages and inflammation can be activated by the influx of free fatty acids (FFAs) and adipokines, such as leptin, from the adipose tissue but also by adipose tissue alterations with macrophage activation and subsequent cytokine secretions that transit to the liver (38). FFAs, in the form of nonesterified fatty acids (NEFAs), are transported from the adipose tissue to the hepatocytes through notably *Cd36* in the liver. However, no modulations of hepatic *Cd36* expression levels or plasma NEFA concentrations in the general circulation were observed. No cytokine or macrophage modification was observed with indole in the subcutaneous adipose tissue, and *ob/ob* mice being leptin deficient, the implication of leptin must be excluded. Thus, the anti-inflammatory and antifibrogenic impact of indole on the liver does not seem to be mediated by adipose tissue molecular influx of FFAs, cytokines, or leptin. Hepatic macrophage activation can also be caused by an enhanced intestinal permeability and endotoxin influx. Indole did not, however, affect intestinal barrier function in *ob/ob* mice unlike previous observations in both germ-free and specific pathogen–free mice submitted to dextran sodium sulfate–induced colitis (20), where the supply of encapsulated indole in the colon enhanced epithelial barrier function. Moreover, no regulation of intestinal inflammation with indole was observed in *ob/ob* mice, unlike previous findings in the small intestine in the context of enteropathy with similar indole dose ranges given by gavage (18). However, *ob/ob* mice did not display altered intestinal barrier function and inflammation compared with control mice, preventing indole treatment from alleviating any deleterious effects. This could be explained by the reduced susceptibility of leptin-deficient mice to intestinal disorders (46), although previous studies have shown alterations in intestinal permeability in these mice (47, 48). It would be of interest to study the impact of a physiological dose of indole on the intestinal barrier in a long-term dietary model of obesity and NAFLD where low-grade endotoxemia is observed, to evaluate the potential indirect effect of indole on liver health. In such a context of diet-induced obesity, indole-3-propionic acid, a bacterial metabolite derived from indole, has been shown to reduce intestinal permeability in mice (49) and reduce plasma endotoxin concentrations in association with reduced lipogenesis, fibrosis, and inflammation in the liver (10). However, in the present study, the expression levels of *Cd14*, toll-like receptor 4 (*Tlr4*), and LPS binding protein (*Lbp*) in the liver, mediating the interaction between LPS and the KCs, were not impacted by indole treatment unlike previous demonstrations ex vivo (8).

Microbial metabolites can also affect cerebral inflammation and behavior (50, 51). Indole can be further metabolized into oxindole and isatin, for instance (52), known to be neurodepressant molecules. Jaglin et al. (16) and Mir et al. (17) have shown in rats that both acute and chronic overproduction of indole increases anxiety-like behavior. However, in our study, with a low dose of indole, we did not observe modulations of markers of inflammation in the brain nor anxiety-like behavior in *ob/ob* mice.

In summary, our results demonstrate the anti-inflammatory and hepatoprotective properties of a chronic administration of a physiological concentration of indole in vivo in a genetic model of obesity and liver steatosis, without impacting on steatosis itself. These modifications appear to be mainly attributable to direct effects of indole on the liver, without any contribution from the adipose tissue or the intestinal barrier. It would be of interest to evaluate the impact of nutritional strategies favoring bacterial indole production on hepatic inflammation in NAFLD.

Acknowledgments

We thank V Allaeys, I Blave, R Selleslagh, and B Es Saadi for their technical support in the project.

The authors' responsibilities were as follows—CK, AMN, and NMD: designed the research; CK, AMN, and SL: conducted the research; QL: analyzed the behavioral test data; PB: analyzed and scored H&E staining; CK, AMN, and NMD: wrote the paper. QL, SL, MB, JR, NL, LBB, and PDC: provided intellectual input and contributed to the writing of the report; NMD: planned and supervised all experiments; and all authors: read and approved the final manuscript.

References

1. Moon AM, Singal AG, Tapper EB. Contemporary epidemiology of chronic liver disease and cirrhosis. Clin Gastroenterol Hepatol 2020;18:2650–66.
2. Knudsen C, Neyrinck AM, Lanthier N, Delzenne NM. Microbiota and nonalcoholic fatty liver disease: promising prospects for clinical interventions? Curr Opin Clin Nutr Metab Care 2019;22(5):393–400.
3. Canfora EE, Meex RCR, Venema K, Blaak EE. Gut microbial metabolites in obesity, NAFLD and T2DM. Nat Rev Endocrinol 2019;15:261–73.
4. Duarte SMB, Stefano JT, Miele L, Ponziani FR, Souza-Basqueira M, Okada L, de Barros Costa FG, Toda K, Mazo DFC, Sabino EC, et al. Gut microbiome composition in lean patients with NASH is associated with

liver damage independent of caloric intake: a prospective pilot study. Nutr Metab Cardiovasc Dis 2018;28(4):369–84.
5. Hoyles L, Fernandez-Real JM, Federici M, Serino M, Abbott J, Charpentier J, Heymes C, Luque JL, Anthony E, Barton RH, et al. Molecular phenomics and metagenomics of hepatic steatosis in non-diabetic obese women. Nat Med 2018;24(7):1070–80.
6. Koh A, Molinaro A, Stahlman M, Khan MT, Schmidt C, Manneras-Holm L, Wu H, Carreras A, Jeong H, Olofsson LE, et al. Microbially produced imidazole propionate impairs insulin signaling through mTORC1. Cell 2018;175(4):947–61.e17.
7. Caussy C, Hsu C, Lo MT, Liu A, Bettencourt R, Ajmera VH, Bassirian S, Hooker J, Sy E, Richards L, et al. Link between gut-microbiome derived metabolite and shared gene-effects with hepatic steatosis and fibrosis in NAFLD. Hepatology 2018;68(3):918–32.
8. Beaumont M, Neyrinck A, Olivares M, Rodriguez J, de Rocca Serra A, Roumain M, Bindels LB, Cani PD, Evenepoel P, Muccioli GG, et al. The gut microbiota metabolite indole alleviates liver inflammation in mice. FASEB J 2018;32(12):6681–93.
9. Krishnan S, Ding Y, Saedi N, Choi M, Sridharan GV, Sherr DH, Yarmush ML, Alaniz RC, Jayaraman A, Lee K. Gut microbiota-derived tryptophan metabolites modulate inflammatory response in hepatocytes and macrophages. Cell Rep 2018;23(4):1099–111.
10. Zhao ZH, Xin FZ, Xue Y, Hu Z, Han Y, Ma F, Zhou D, Liu XL, Cui A, Liu Z, et al. Indole-3-propionic acid inhibits gut dysbiosis and endotoxin leakage to attenuate steatohepatitis in rats. Exp Mol Med 2019;51:1–14.
11. Ji Y, Gao Y, Chen H, Yin Y, Zhang W. Indole-3-acetic acid alleviates nonalcoholic fatty liver disease in mice via attenuation of hepatic lipogenesis, and oxidative and inflammatory stress. Nutrients 2019;11:2062.
12. Jin UH, Lee SO, Sridharan G, Lee K, Davidson LA, Jayaraman A, Chapkin RS, Alaniz R, Safe S. Microbiome-derived tryptophan metabolites and their aryl hydrocarbon receptor-dependent agonist and antagonist activities. Mol Pharmacol 2014;85(5):777–88.
13. Dong F, Hao F, Murray IA, Smith PB, Koo I, Tindall AM, Kris-Etherton PM, Gowda K, Amin SG, Patterson AD, et al. Intestinal microbiota-derived tryptophan metabolites are predictive of Ah receptor activity. Gut Microbes 2020;12(1):1788899.
14. Karlin DA, Mastromarino AJ, Jones RD, Stroehlein JR, Lorentz O. Fecal skatole and indole and breath methane and hydrogen in patients with large bowel polyps or cancer. J Cancer Res Clin Oncol 1985;109(2):135–41.
15. Zuccato E, Venturi M, Di Leo G, Colombo L, Bertolo C, Doldi SB, Mussini E. Role of bile acids and metabolic activity of colonic bacteria in increased risk of colon cancer after cholecystectomy. Digest Dis Sci 1993;38(3):514–9.
16. Jaglin M, Rhimi M, Philippe C, Pons N, Bruneau A, Goustard B, Dauge V, Maguin E, Naudon L, Rabot S. Indole, a signaling molecule produced by the gut microbiota, negatively impacts emotional behaviors in rats. Front Neurosci 2018;12:216.
17. Mir H-D, Milman A, Monnoye M, Douard V, Philippe C, Aubert A, Castanon N, Vancassel S, Guérineau NC, Naudon L, et al. The gut microbiota metabolite indole increases emotional responses and adrenal medulla activity in chronically stressed male mice. Psychoneuroendocrinology 2020;119:104750.
18. Whitfield-Cargile CM, Cohen ND, Chapkin RS, Weeks BR, Davidson LA, Goldsby JS, Hunt CL, Steinmeyer SH, Menon R, Suchodolski JS, et al. The microbiota-derived metabolite indole decreases mucosal inflammation and injury in a murine model of NSAID enteropathy. Gut Microbes 2016;7(3):246–61.
19. Bansal T, Alaniz RC, Wood TK, Jayaraman A. The bacterial signal indole increases epithelial-cell tight-junction resistance and attenuates indicators of inflammation. Proc Natl Acad Sci U S A 2010;107(1):228–33.
20. Shimada Y, Kinoshita M, Harada K, Mizutani M, Masahata K, Kayama H, Takeda K. Commensal bacteria-dependent indole production enhances epithelial barrier function in the colon. PLoS One 2013;8(11).
21. Chimerel C, Emery E, Summers DK, Keyser U, Gribble FM, Reimann F. Bacterial metabolite indole modulates incretin secretion from intestinal enteroendocrine L cells. Cell Rep 2014;9(4):1202–8.
22. Ma L, Li H, Hu J, Zheng J, Zhou J, Botchlett R, Matthews D, Zeng T, Chen L, Xiao X, et al. Indole alleviates diet-induced hepatic steatosis and inflammation in a manner involving myeloid cell PFKFB3. Hepatology 2020;72:1191–1203.
23. Lee JH, Lee J. Indole as an intercellular signal in microbial communities. FEMS Microbiol Rev 2010;34(4):426–44.
24. Lanthier N, Molendi-Coste O, Horsmans Y, van Rooijen N, Cani PD, Leclercq IA. Kupffer cell activation is a causal factor for hepatic insulin resistance. Am J Physiol Gastrointest Liver Physiol 2010;298(1):G107–16.
25. Reeves PG, Nielsen FH, Fahey GC, Jr. AIN-93 purified diets for laboratory rodents: final report of the American Institute of Nutrition ad hoc writing committee on the reformulation of the AIN-76A rodent diet. J Nutr 1993;123(11):1939–51.
26. Yalkowsky SH, Dannenfelser RM. Aquasol database of aqueous solubility. Tucson (AZ): College of Pharmacy, University of Arizona; 1992.p. 189.
27. Neyrinck AM, Possemiers S, Verstraete W, De Backer F, Cani PD, Delzenne NM. Dietary modulation of clostridial cluster XIVa gut bacteria (Roseburia spp.) by chitin-glucan fiber improves host metabolic alterations induced by high-fat diet in mice. J Nutr Biochem 2012;23(1):51–9.
28. Rohart F, Gautier B, Singh A, Le Cao KA. mixOmics: an R package for 'omics feature selection and multiple data integration. PLoS Comput Biol 2017;13(11):e1005752.
29. Cao K-AL, Rohart F, Gonzalez I, Dejean S. mixOmics: omics data integration project. R package version 6.12.1 [Internet]. 2021; [cited 2021 Jan 21]. Available from: http://www.bioconductor.org/packages/release/bioc/html/mixOmics.html.
30. Liu T, Zhang L, Joo D, Sun S-C. NF-κB signaling in inflammation. Sig Transduct Target Ther 2017;2(1):17023.
31. Nakatsumi H, Matsumoto M, Nakayama KI. Noncanonical pathway for regulation of CCL2 expression by an mTORC1-FOXK1 axis promotes recruitment of tumor-associated macrophages. Cell Rep 2017;21(9):2471–86.
32. Wada T, Sunaga H, Miyata K, Shirasaki H, Uchiyama Y, Shimba S. Aryl hydrocarbon receptor plays protective roles against high fat diet (HFD)-induced hepatic steatosis and the subsequent lipotoxicity via direct transcriptional regulation of Socs3 gene expression. J Biol Chem 2016;291(13):7004–16.
33. Natividad JM, Agus A, Planchais J, Lamas B, Jarry AC, Martin R, Michel M-L, Chong-Nguyen C, Roussel R, Straube M, et al. Impaired aryl hydrocarbon receptor ligand production by the gut microbiota is a key factor in metabolic syndrome. Cell Metab 2018;28:737–49.
34. Finger BC, Dinan TG, Cryan JF. Leptin-deficient mice retain normal appetitive spatial learning yet exhibit marked increases in anxiety-related behaviours. Psychopharmacology (Berl) 2010;210(4):559–68.
35. Rothhammer V, Mascanfroni ID, Bunse L, Takenaka MC, Kenison JE, Mayo L, Chao CC, Patel B, Yan R, Blain M, et al. Type I interferons and microbial metabolites of tryptophan modulate astrocyte activity and central nervous system inflammation via the aryl hydrocarbon receptor. Nat Med 2016;22(6):586–97.
36. Lukacs-Kornek V, Schuppan D. Dendritic cells in liver injury and fibrosis: shortcomings and promises. J Hepatol 2013;59(5):1124–6.
37. Itoh M, Suganami T, Kato H, Kanai S, Shirakawa I, Sakai T, Goto T, Asakawa M, Hidaka I, Sakugawa H, et al. CD11c+ resident macrophages drive hepatocyte death-triggered liver fibrosis in a murine model of nonalcoholic steatohepatitis. JCI Insight 2017;2(22):e92902.
38. Kazankov K, Jorgensen SMD, Thomsen KL, Moller HJ, Vilstrup H, George J, Schuppan D, Gronbaek H. The role of macrophages in nonalcoholic fatty liver disease and nonalcoholic steatohepatitis. Nat Rev Gastroenterol Hepatol 2019;16(3):145–59.
39. Marra F, Tacke F. Roles for chemokines in liver disease. Gastroenterology 2014;147(3):577–94.e1.
40. Lee UE, Friedman SL. Mechanisms of hepatic fibrogenesis. Best Pract Res Clin Gastroenterol 2011;25(2):195–206.
41. Xu R, Huang H, Zhang Z, Wang F-S. The role of neutrophils in the development of liver diseases. Cell Mol Immunol 2014;11(3):224–31.
42. Hendrikx T, Schnabl B. Indoles: metabolites produced by intestinal bacteria capable of controlling liver disease manifestation. J Intern Med 2019;286(1):32–40.

43. Hubbard TD, Murray IA, Perdew GH. Indole and tryptophan metabolism: endogenous and dietary routes to Ah receptor activation. Drug Metab Dispos 2015;43(10):1522–35.
44. Hubbard TD, Murray IA, Bisson WH, Lahoti TS, Gowda K, Amin SG, Patterson AD, Perdew GH. Adaptation of the human aryl hydrocarbon receptor to sense microbiota-derived indoles. Sci Rep 2015;5: 12689.
45. Obstfeld AE, Sugaru E, Thearle M, Francisco AM, Gayet C, Ginsberg HN, Ables EV, Ferrante AW, Jr. C-C chemokine receptor 2 (CCR2) regulates the hepatic recruitment of myeloid cells that promote obesity-induced hepatic steatosis. Diabetes 2010;59(4): 916–25.
46. Siegmund B, Lehr HA, Fantuzzi G. Leptin: a pivotal mediator of intestinal inflammation in mice. Gastroenterology 2002;122(7): 2011–25.
47. Brun P, Castagliuolo I, Di Leo V, Buda A, Pinzani M, Palu G, Martines D. Increased intestinal permeability in obese mice: new evidence in the pathogenesis of nonalcoholic steatohepatitis. Am J Physiol Gastrointest Liver Physiol 2007;292(2):G518–25.
48. Cani PD, Possemiers S, Van de Wiele T, Guiot Y, Everard A, Rottier O, Geurts L, Naslain D, Neyrinck A, Lambert DM, et al. Changes in gut microbiota control inflammation in obese mice through a mechanism involving GLP-2-driven improvement of gut permeability. Gut 2009;58(8):1091–103.
49. Jennis M, Cavanaugh CR, Leo GC, Mabus JR, Lenhard J, Hornby PJ. Microbiota-derived tryptophan indoles increase after gastric bypass surgery and reduce intestinal permeability in vitro and in vivo. Neurogastroenterol Motil [Internet] 2018;30(2). doi:10.1111/nmo.13178.
50. Torres-Fuentes C, Schellekens H, Dinan TG, Cryan JF. The microbiota-gut-brain axis in obesity. Lancet Gastroenterol Hepatol 2017;2(10):747–56.
51. O'Mahony SM, Clarke G, Borre YE, Dinan TG, Cryan JF. Serotonin, tryptophan metabolism and the brain-gut-microbiome axis. Behav Brain Res 2015;277:32–48.
52. Lee JH, Wood TK, Lee J. Roles of indole as an interspecies and interkingdom signaling molecule. Trends Microbiol 2015;23(11): 707–18.